UNIVERSITY OF AMSTERDAM

UvA-DARE (Digital Academic Repository)

X-shooter near-IR spectrograph arm realisation

Navarro, R.; Elswijk, E.; Tromp, N.; ter Horst, R.; Horrobin, M.; Vernet, J.; Finger, G.; Groot, P.; Kaper, L.

DOI
10.1117/12.789778

Publication date
2008

Document Version
Author accepted manuscript

Published in
Ground-based and Airborne Instrumentation for Astronomy II

Link to publication

Citation for published version (APA):
Navarro, R., Elswijk, E., Tromp, N., ter Horst, R., Horrobin, M., Vernet, J., Finger, G., Groot, P., & Kaper, L. (2008). X-shooter near-IR spectrograph arm realisation. In I. S. McLean, & M. M. Casali (Eds.), *Ground-based and Airborne Instrumentation for Astronomy II: 23-28 June 2008, Marseille, France* (Vol. 2). Article 70141Y (Proceedings of SPIE, the International Society for Optical Engineering; Vol. 7014). SPIE. https://doi.org/10.1117/12.789778

General rights
It is not permitted to download or to forward/distribute the text or part of it without the consent of the author(s) and/or copyright holder(s), other than for strictly personal, individual use, unless the work is under an open content license (like Creative Commons).

Disclaimer/Complaints regulations
If you believe that digital publication of certain material infringes any of your rights or (privacy) interests, please let the Library know, stating your reasons. In case of a legitimate complaint, the Library will make the material inaccessible and/or remove it from the website. Please Ask the Library: https://uba.uva.nl/en/contact, or a letter to: Library of the University of Amsterdam, Secretariat, P.O. Box 19185, 1000 GD Amsterdam, The Netherlands. You will be contacted as soon as possible.

UvA-DARE is a service provided by the library of the University of Amsterdam (https://dare.uva.nl)

Download date:10 Oct 2026

X-shooter Near-IR Spectrograph Arm Realisation

Ramon Navarro [a], Eddy Elswijk [a], Niels Tromp [a], Rik ter Horst [a], Matthew Horrobin [c],
Joel Vernet [d], Gert Finger [d], Paul Groot [b], Lex Kaper [c]
[a] NOVA-ASTRON, P.O. Box 2, Dwingeloo, Netherlands
[b] Radboud University Nijmegen, P.O. Box 9010, Nijmegen, Netherlands
[c] University of Amsterdam, Kruislaan 403, Amsterdam, Netherlands
[d] ESO, Karl-Schwarzschild-Strasse 2, Garching, Germany

ABSTRACT

X-shooter is a new high-efficiency spectrograph observing the complete spectral range of 300-2500 nm in a single exposure, with a spectral resolving power R>5000. The instrument will be located at the Cassegrain focus of one of the VLT UTs and consists of three spectrographs: UV, VIS and Near-IR. This paper addresses the design, hardware realization and performance of the Near-IR spectrograph of the X-Shooter instrument and its components.

Various optical, mechanical and cryogenic manufacturing and verification techniques are discussed. The cryogenic performance of replicated light weight gratings is presented. Bare aluminium mirrors are produced and polished to optical quality to preserve high shape accuracy at cryogenic conditions. Their manufacturing techniques and performance are both discussed. The cryogenic collimator and dispersion boxes, on which the optical components are mounted, feature integrated baffles for improved stiffness and integrated leaf springs to reduce tension on optical components, thereby challenging 5 axis simultaneous CNC milling capabilities. ASTRON Extreme Light Weighting is used for a key component to reduce the flexure of the cryogenic system; some key numbers and unique manufacturing experience for this component are presented. The method of integrated system design at cryogenic working temperatures and the resulting alignment-free integration are evaluated. Finally some key lab test results for the complete NIR spectrograph are presented.

Keywords: X-shooter, spectrograph, infrared, cryogenic, design at operating temperature, ASTRON extreme light-weighting, polished aluminium mirror

1. INTRODUCTION

X-shooter is a single target, wide-band medium resolution spectrograph for the VLT. The wavelength range is 0.3 to 2.5 µm i.e. from the UV to the IR including the K-band. X-shooter is a Cassegrain focus instrument with only two observing modes (direct slit, image slicer) and a fixed spectral format [Ref. 1 & 2].

The instrument consists of a central structure (the Backbone) onto which three spectrographs are mounted that cover the UV-Blue, VISible and Near InfraRed (NIR) spectral ranges. The Backbone contains the calibration system, Acquisition and Guiding camera, dichroics to split the light from the telescope in three wavelength bands and Atmospheric Dispersion Correctors (ADC) for the UVB and VIS arms, see figure 1. Active mirrors compensate for flexure inside the backbone and keep the three slits aligned.

The focus of this paper is on the realization of the NIR Spectrograph. The NIR Spectrograph is cooled with a liquid nitrogen bath cryostat as closed cycle coolers may cause unwanted vibrations. The instrument operates at 105 Kelvin, while the detector is cooled to 81 Kelvin. Note that the cryogenic and thermal design of the X-shooter NIR Spectrograph is not covered in this paper, but in the same conference in paper [Ref. 3].

As X-shooter is located at the Cassegrain focus it suffers from a changing direction of the gravity vector. By using light-weighted mirrors and a light-weighted mechanical structure the stiffness to weight ratio is optimized, which allows the instrument to be built just inside the VLT mass limit of 2.5 ton. The suspension of the NIR Cold Optics box inside the cryostat is done with three titanium rods, combining strength (earthquakes) and stiffness with a low heat load. The cryostat diameter is 1200 mm, its mass is 550 kg, including the cold bench.

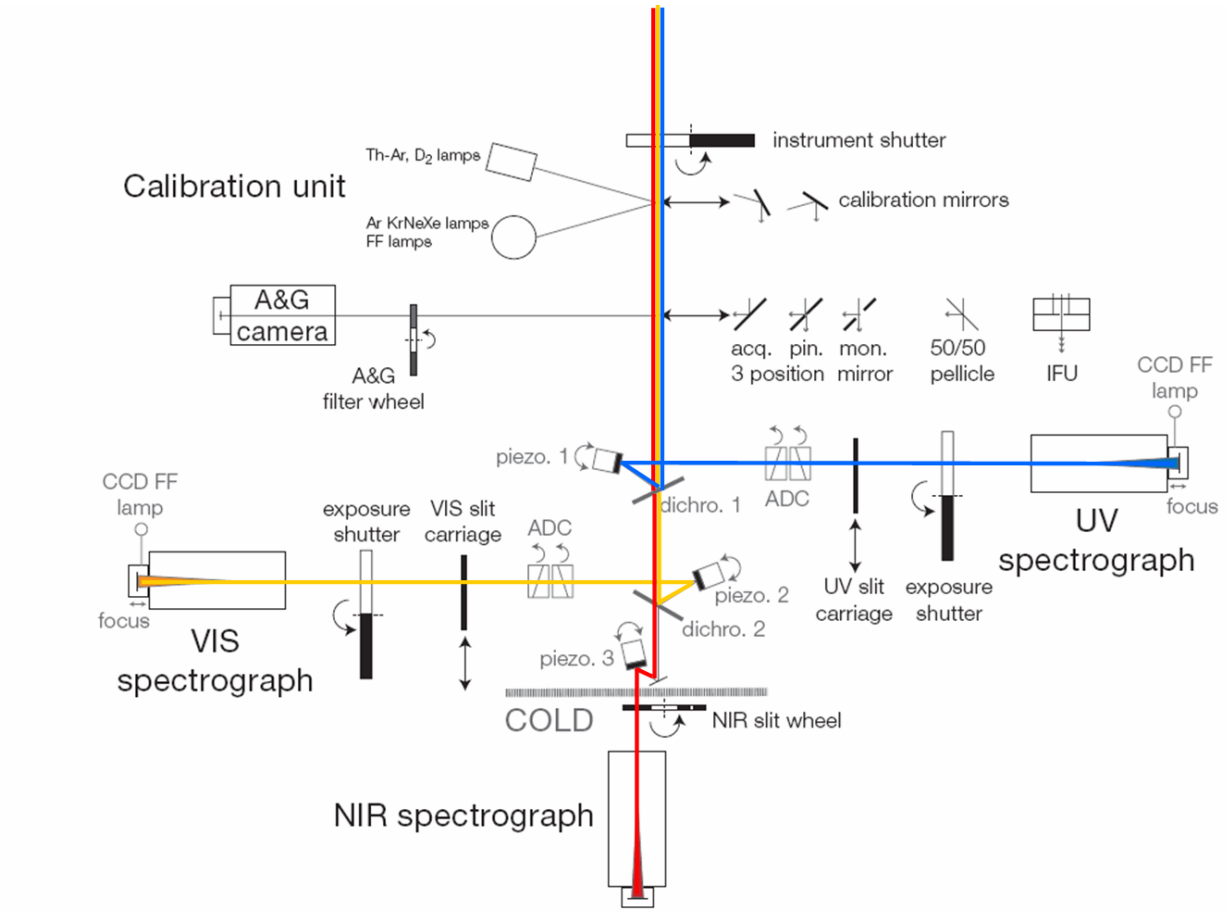

Figure 1. Schematic view of X-shooter

The optical design of the X-shooter NIR Spectrograph foresees two uncooled dichroics and two image relay mirrors that re-image the Cassegrain focus on a slit inside the cryostat. From the slit the light passes the collimator and enters the dispersion box, consisting of an echelle grating in near-Littrow configuration for the main dispersion and three prisms in double pass for the cross dispersion. The light passes the collimator again, enters the camera and reaches the detector [Ref. 4]. The cold optics box is shown in figure 2.

2. MANUFACTURE

The entire assembly of the cold optical box is designed at an operational temperature of 105 K. This is necessary to know the exact location of the interfaces between all the components and assemblies, especially if various materials with different Coefficient of Thermal Expansion (CTE) are used. The V-rods have been modeled separately, because of the temperature gradient from 105 K to 300 K over the structure. Additionally, the shrink of the optical box during cool down deforms the V-rods and thus lifts the optical box a few mm.

In the design phase individual components are digitally warmed to room temperature in order to model standard sized bolts and dowel pins. For aluminium parts all dimensions increase by 0.36%. The transition from operational temperature to room temperature is performed in the mechanical design software Pro/Engineer as the optical design software ZEMAX is not fit to perform the 3D calculations needed. Note that the temperature transition for optical properties is done in ZEMAX, for instance radius and aspheric parameters [Ref. 5]. The temperature transition process is automated, but still requires a good administration of the temperature of the component under design. Manufacturing drawings are also at room temperature, which is the environment for fabrication and verification of dimensions.

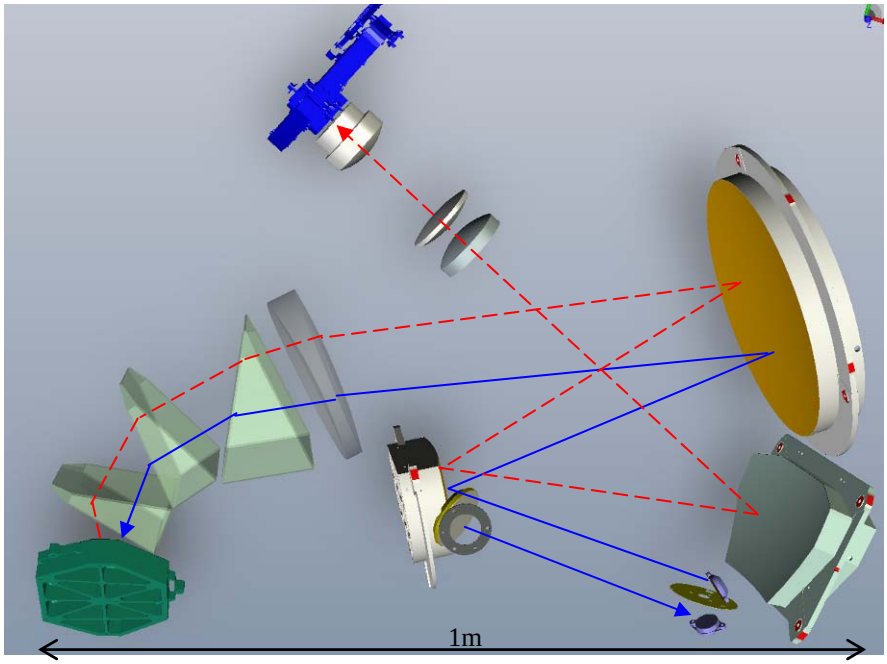

Figure 2. Schematic view of the cold optics in the X-shooter near infrared spectrograph. The Cassegrain focus and the warm re-imaging optics are situated above the plane of the paper (not shown). The cryostat entrance window and cold stop are located just below the center. The slit wheel is located in the lower right. The light beam passes two collimator mirrors (center and right) and enters the dispersion box on the left [blue, solid line]. The dispersion box consists of three prisms and an echelle grating. On the return path the light passes the collimator again, enters the camera and hits the detector in the upper left [red, dashed line].

The grating (∅ 150mm) and larger mirrors used in the X-shooter NIR Spectrograph (optical surface ∅ 160, 260 and 300 mm) are conventionally light-weighted (open back) in order to reduce mass, while improving the mass to stiffness ratio. An elaborate heat treatment process is used in order to minimize global deformation by aging in time. The process consists of CNC milling the component with an oversize of 1mm, followed by solution treatment and down- and up-hill quenching for full recrystallization of the material (Aluminium T6 treatment). In a second CNC milling step the component is milled to the final size, with only some extra material on the optical surface, followed by aging. A third CNC Milling step reduces the oversize on the optical surfaces to only a few tens of micrometers, followed by several thermal cycles. This procedure should limit internal stress deformations of the optical surface to only a few nanometer, even at cryogenic temperatures. The last step is to replicate the grating on the surface, or for the mirrors the bare aluminium surface is directly polished to optical specifications [figure 3]. This technique has been developed at ASTRON and has a greatly improved surface roughness over diamond turning, because it does not suffer from the grating effect [Ref. 5].

Extreme light weighting has been used to produce the aluminium balance arm, a stiff device that holds the cold optics box while minimizing its flexure under gravity variation. Compared to conventional light-weighting techniques the new technique allows for light-weighting percentages of over 90% while at the same time increasing stiffness in bending and torsion by more than 50% [Ref. 6 & 7]. A high degree of light-weighting requires full control over the five degrees of freedom in the milling machine. Large internal volumes (pockets) are created by milling through small entrance holes. ASTRON has developed various techniques to improve the efficiency of excavating large internal volumes through a relatively small entrance hole. Two balance arms have been produced with different techniques. In the plunging technique the CNC mill drills through a single opening hole at many different angles, while the spooning technique is similar to excavating a coconut with a spoon through a small opening.

The Collimator Box and the Dispersion Box are manufactured from a single solid block of 850 kg aluminium. The inside of the boxes is immediately manufactured to final dimensions using wire spark erosion in a scalp pattern to reduce the impact of possible stray light. The walls are 100mm thick before both boxes are CNC milled to the desired shape from the outside only. The heat treatment process is elaborate in order to minimize global deformation by aging in time. The

process consists of CNC milling the component with an oversize of 1mm, followed by aging. In a second CNC milling step the component is milled to size, with only some extra material on the mounting surfaces, followed by several thermal cycles. A third CNC milling step only addresses the mounting surfaces. This procedure should limit internal stress deformations of the optical surface to only a few micrometer, even at cryogenic temperatures. The whole procedure took 3 months of exclusive CNC machine time and was performed in house at NOVA-ASTRON. The largest error of all mounting positions on the collimator box is a mere 7 micrometer.

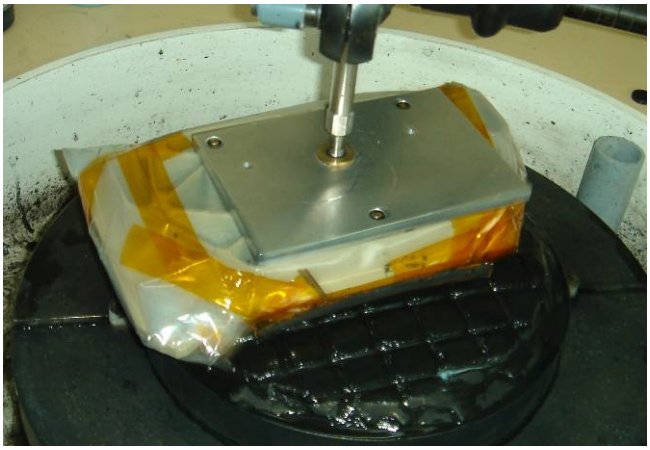

Figure 3. In a newly developed technique the bare aluminium mirror is conventionally polished to optical quality, The mirror is wrapped in plastic to avoid contamination during polishing. Achieved surface figures are <200nm together with a surface roughness in the order of 1nm.

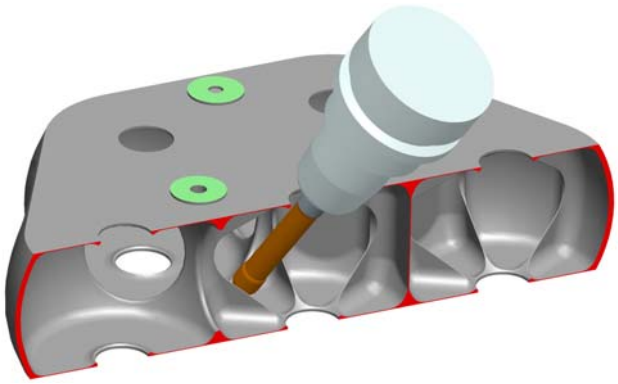

Figure 4. Balance Arm using the ASTRON extreme light-weighting technique. Large internal volumes (pockets) are created by milling through small entrance holes. The weight of the 540 x 400 x 57 mm aluminium balance arm is 2kg, which corresponds to lightweighting percentage of 90%. Internal ribs in the pockets improve the overall stiffness.

The number of interfaces on the collimator box is very high due to the many components to be mounted on the box. The inside box is painted black to reduce stray light, except for mounting surfaces [figure 5]. Mirror mounting pads are located on integrated spring blades in order not to induce stress on the mirrors due to internal stress or temperature variations in the box. For the same reason the mirrors are mounted using a torx free mounting system. The force induced by a package of conical spring washers holds the mirror in place. The package of conical spring washers is positioned by releasing three clamp tools simultaneously. Using this method the mirrors are mounted without the need for (high) rotational forces as common when tightening bolts. Another complication for the optical box is the lack of space between optical components. To reduce deformations of the optical box it was necessary to use integrated baffles as structural components of the collimator box [figure 6].

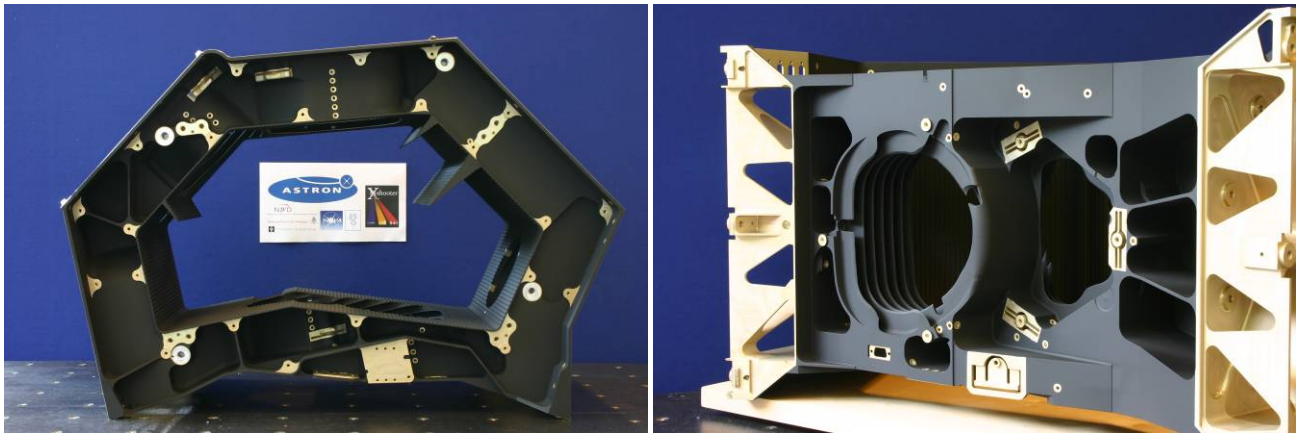

Figure 5. The 25kg, 800 x 540 x 400 mm, aluminium cold optics collimator box is coated with alodine (gold color) and painted black to reduce stray light, except for mounting surfaces. The cold optics collimator box has integrated baffles and spring leafs to mount the mirrors (right).

The weight of the completed collimator box is 25kg, the dispersion box adds 12kg. Both boxes are covered with two lids weighting 6kg each. This brings the size of the structure to 950 x 780 x 400 mm and the mass to 49kg. The weight of the final assembly is 120kg, including titanium V-rods suspension, copper braids for cooling and all optical components.

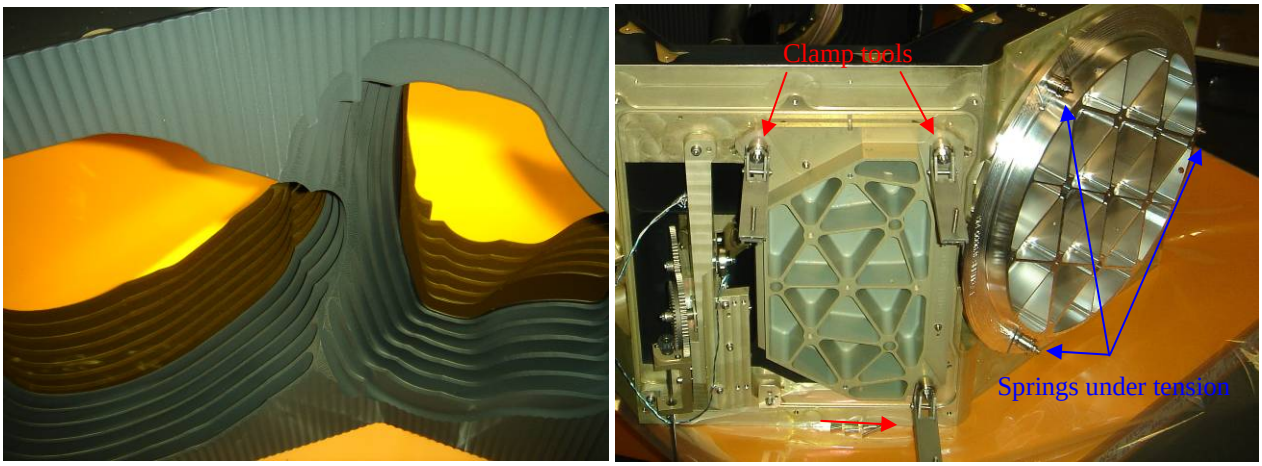

Figure 6. The two largest mirrors (M7 & M8) mounted in the cold optics collimator box. Baffles are created in the wall of the box as structural elements in order to minimize flexure deformation. The baffles are also reflected in the gold coated mirrors (left image). The mirrors are mounted on springs in the collimator box with a torx free mounting system (right image). At the right M7 has been mounted, M8 in the center is being mounted with clamp 3 tools.

3. ASSEMBLY AND INTEGRATION

After integration of the mirrors and the slit wheel in the collimator box, the optical performance of the collimator is tested in double pass using white light, a dummy camera (cylindrical nullens) and a CCD detector. The dispersive elements are mimicked by a flat mirror, since these optics are crossed with an almost collimated beam Intra- and extra-focal images indicate an optical performance of the system that behaves as predicted by the ZEMAX model.

Birefringence effects in the prisms have been investigated using crossed polarizers. The clamping force on the prism must be delicately balanced to distribute the force evenly over the pads in order to minimize stress birefringence [figure 8]. Wave front data of the three prisms in double pass was taken in order to verify the functional performance of the assembly. The wave front has a cloudy appearance in the interferogram, probably due to local variations in the index of refraction inside the ZnSe material. Stress induced birefringence can even cancel interference at the location of the mounting pads.

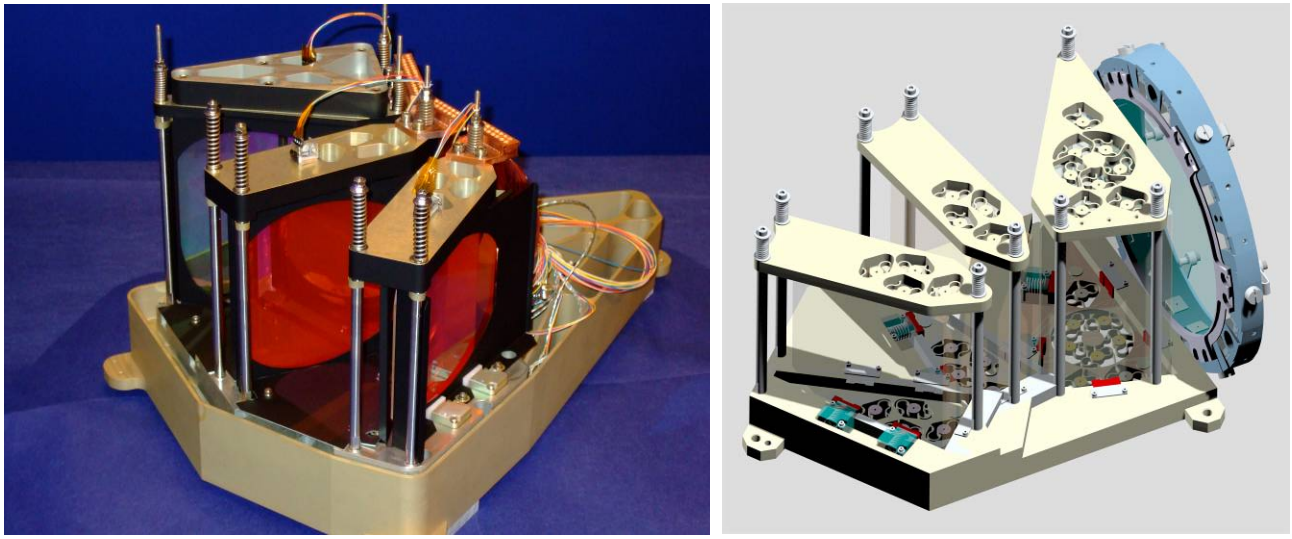

Figure 7. The assembled prism bench includes baffles at each prism surface. Copper braids and thermal conduction spring pads provide symmetrical cooling of the prisms and distribute mechanical force to reduce stress induced birefringence. CTE compensation elements keep the prisms at the desired location at any temperature.

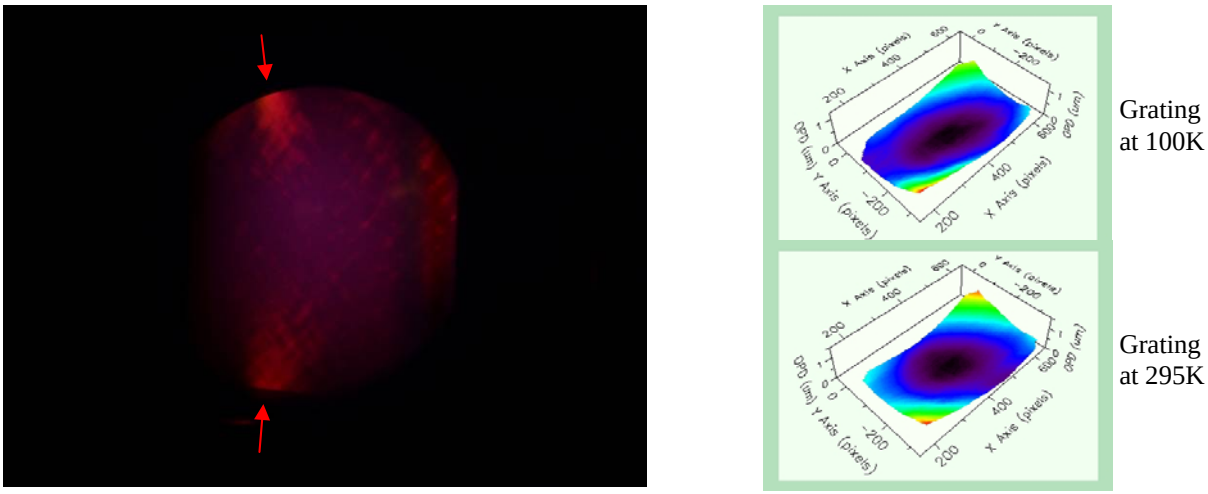

Figure 8. Stress induced birefringence effects in the prisms have been observed when the clamping force is not distributed evenly over the prism (left). The location of mounting pads is indicated by the red arrows. Cryogenic wavefront performance of the replicated test grating: 134 nm RMS at 100 K and 155 nm RMS at 295 K (right).

The optical performance of the grating was inspected at cryogenic temperatures. Wave front variation was investigated in particular, because the risk of bimetallic effects in the grating by the thick resin layer holding the replicated grating pattern. Variation in the wave front data between the warm and cold situation is dominated by thermal lensing of the cryostat window. There is no print through of the open back lightweight structure. No flaking or peeling of the resin layer or gold coating was observed.

All components are mounted in the dispersion box at manufacturing tolerances without need for alignment. Also the Camera and Detector are integrated on the collimator box without need for alignment. The only adjustment that was done is to tilt the detector by 1 mm (the largest tilt possible) with the intention that the image would be perfectly focused at some location on the detector, see test results section.

Thermal sensors were glued directly on the corrector lens, the infrasil prism (P1) and the last camera lens (L3), since these optical element are the slowest and most critical during warm up / cool down.

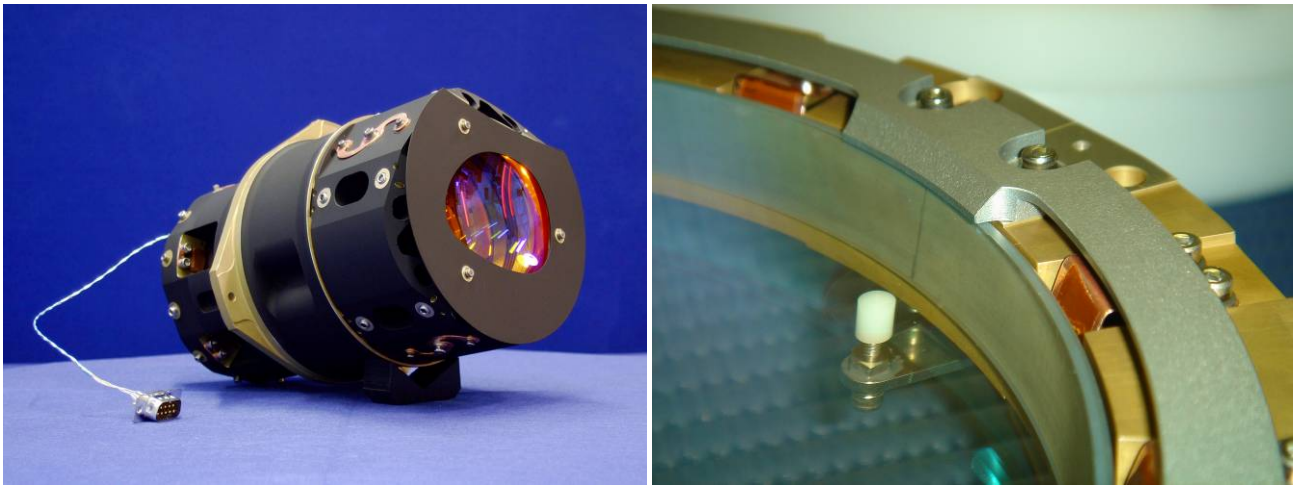

Figure 9. The Camera consists of 2 ZnSe aspheres and 1 CaF2 asphere (Left image). All lenses are mounted using CTE compensation mechanisms in order to maintain accurate alignment at both room temperature and operating temperature. Copper spring pads plated with indium are used for a fast cool down and warm up and are clearly visible in the detail of the corrector lens mount in the right image.

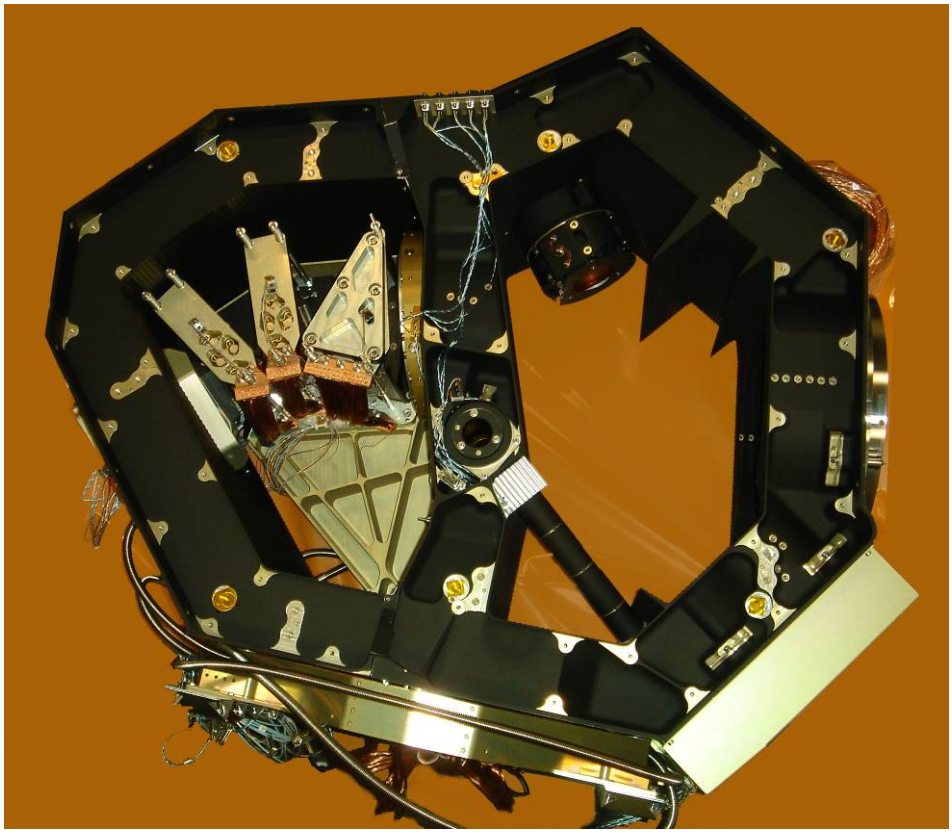

Figure 10. The integrated Cold Optics Box before closing the lids. The light enters the optics box through the cold stop at the center of the image. The light is deflected through a light tight tunnel to the slit wheel located in a light tight box at the lower right. From there the light travels correspondingly to M6 (underneath the cold stop), M7 at the extreme right and the corrector lens (above the cold stop), where the light enters the dispersion box. The prisms are located at the top left and the grating is located at the far left. The return beam eventually hits M8 at the lower right and the camera and detector at the top op the collimator box. The balance arm is visible at the bottom and the V-Rods are mounted after closing the lids.

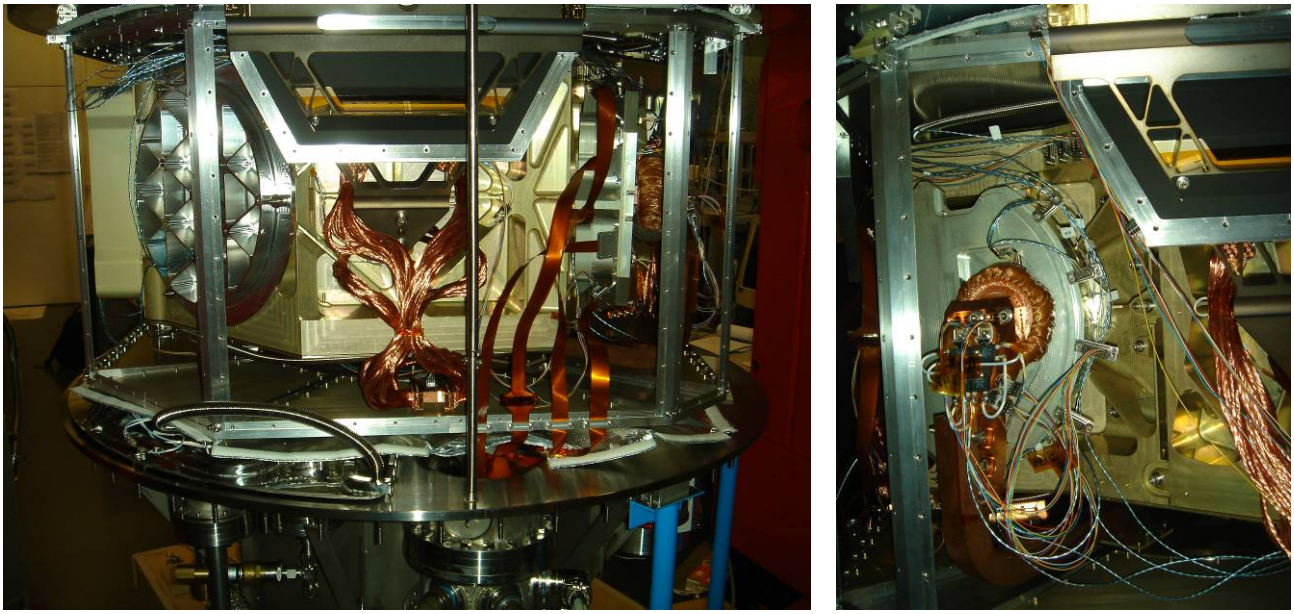

Figure 11. The Cold Optics Box integrated in the cryostat before closing the heat shield. M7 is visible at the left. In the center is a V-Rod including a light tight meander and copper braids for cooling by conducting the ambient heat input from the V-Rods to the liquid nitrogen tank at the bottom of the image The connection with the instrument is also the location where the temperature of the instrument is stabilized to 105.0 +/- 0.1 K. The detector is at the right with 4 flat cables coming from the vacuum feed through. In the right image a detail of the detector housing and cooling is shown. 50 kg of copper is used to cool the instrument and most of it is needed to cool the detector. The detector temperature is stabilized to 81.000 +/- 0.010 K (sea-level) at any orientation of the instrument (telescope) and at any level of liquid nitrogen in the tank. At the VLT the detector can probably run at 80 Kelvin due to the lower boiling temperature of LN2 at higher altitudes.

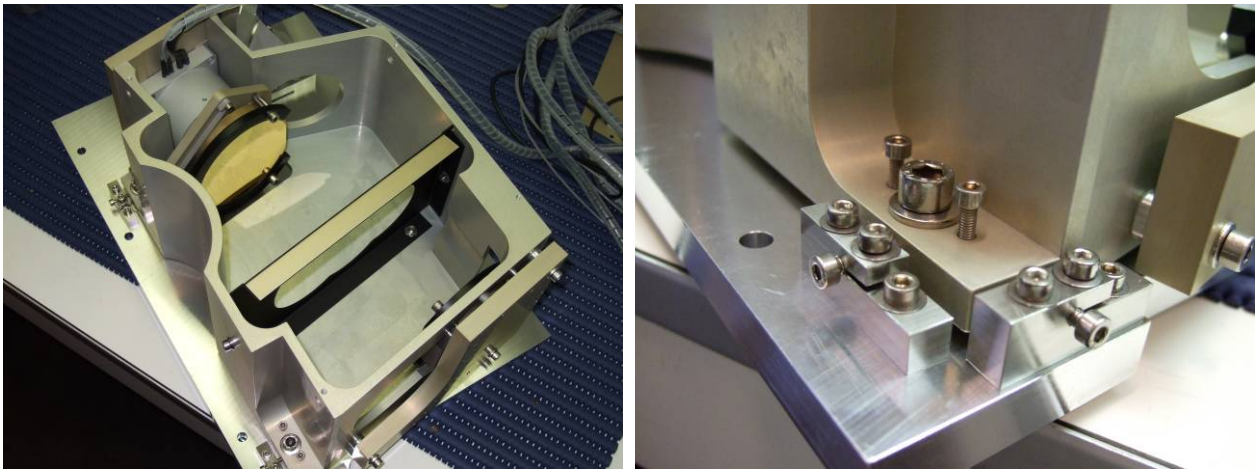

Figure 12. The warm Optics Box (right picture) integrated, before closing the lid. All positioning bolts that enable 6 degrees of freedom (left picture)are set to its nominal position, resulting in an immediate well aligned cryostat with respect to the warm pre optics. Clearly visible on the left upper position is the piezo-controlled flexure compensator. The warm pre-optics mirrors could only be tested in assembly, due to the long radii of curvature.

After thorough checks of all electrical connections, the heat shield is closed, MLI applied, surplus cable length that prevent heat load on the cold instrument are strapped up and the cylindrical wall closes the NIR-arm. The instrument is ready for purging, pumping and cooling.

4. TEST RESULTS

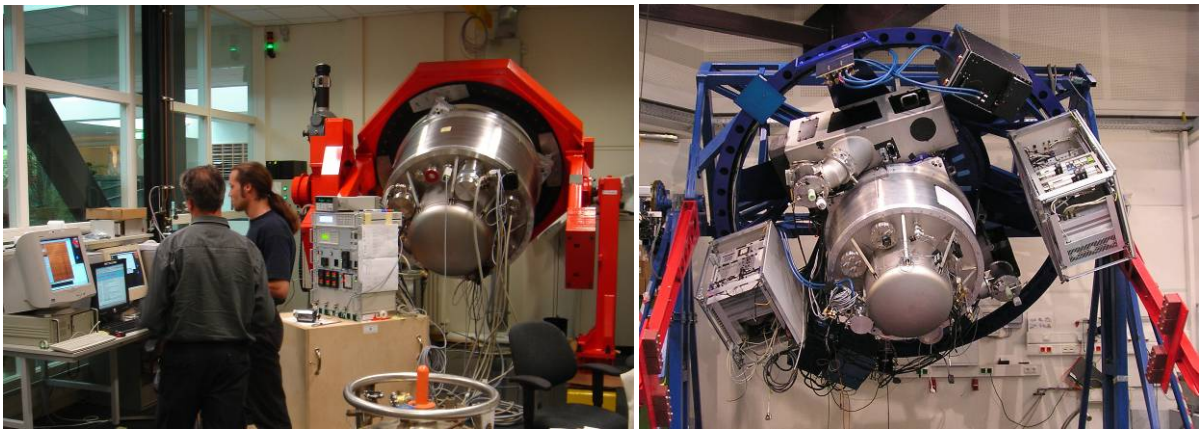

Figure 13. X-shooter near infrared spectrograph during tests at NOVA-ASTRON (left image). The cryostat is mounted on a dummy backbone that is mounted on the telescope simulator (right). The Cold Optical Box is located inside the cryostat. Other equipment comprise the cryogenic control electronics (center) and 3 workstations to control the detector, run the VLT software and analyze all data. The top of one of six liquid nitrogen tanks is visible in the front. X-shooter integrated with the backbone, UVB and VIS spectrographs and electronics in the ESO lab (right image).

At the end of 2007 the milestone of first laboratory light was achieved. For the first time the entire system was assembled and being tested at an operational temperature of 105 K. Within seconds a clear image of the infrared spectrum of the room lights was revealed (figure 14). At one side of the image the focus was excellent allowing to judge image quality and thereby the spectrometer performance immediately. As explained earlier, the detector had been tilted deliberately with respect to the optical axis in order to scan trough focus without the need for additional time consuming cool-downs.

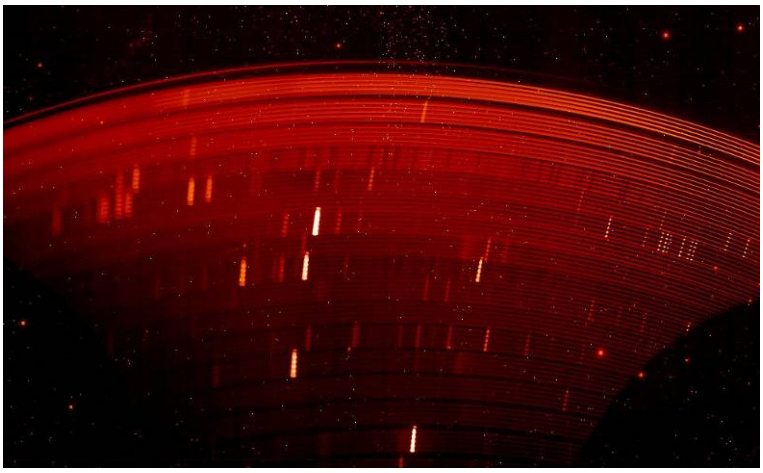

Figure 14. X-shooter NIR spectrum at first laboratory light. At the right of the image the focus is excellent. The detector was tilted deliberately with respect to the optical axis in order to scan trough focus without the need for additional time consuming cool-down runs. The light source is the TL lightning in the lab.

In March 2008 the spectrograph was accepted by the consortium after a record breaking low of only 5 cool-down runs. These cool-down runs were needed for upgrades (grating, sorption pump and electronics), repairs (slit wheel drive and vacuum system) and various tests (temperature sensors and flexure in different configurations). After arrival of the instrument at ESO Garching, before integration with the X-shooter backbone and VIS and UVB spectrographs, ASTRON people upgraded the slit wheel and upgraded and refocused the detector.

The excellent image quality (figure 15) is reflected in the spectral resolution, that is better than specified. With a slit of 0.6 arcseconds width the spectral resolution is between 8500 and 9500, while for a slit of 1.0 arcseconds width the spectral resolution is between 6000 and 6600 (figure 16).

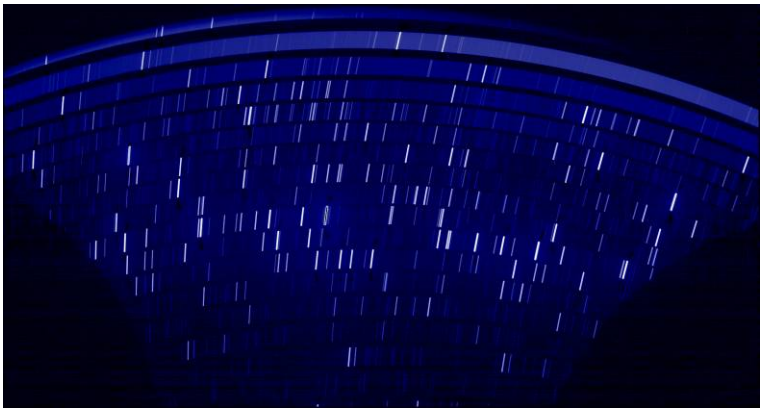

Figure 15. X-shooter NIR Th-Ar spectrum at preliminary acceptance Europe.

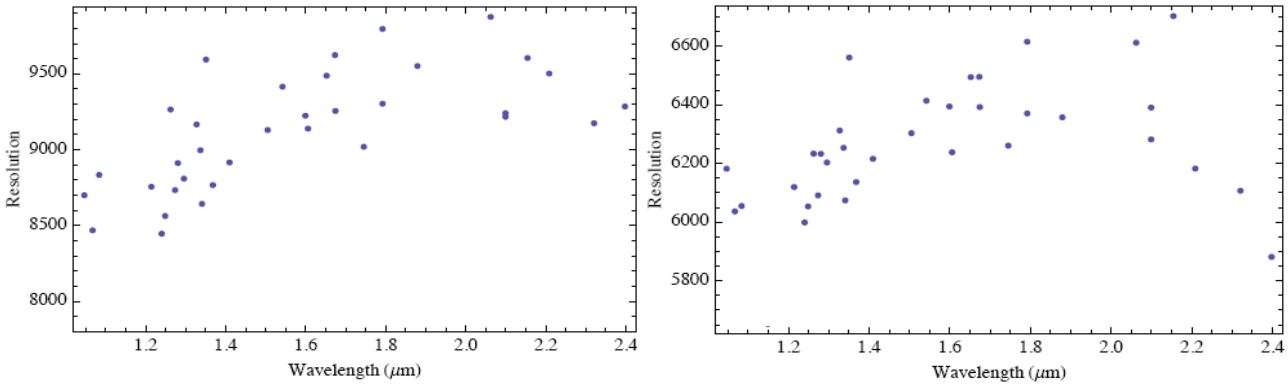

Figure 16. Spectral resolution measured with slit width of 0.6 arcsecond (left) and 1.0 arcsecond (right).

The main goal of X-shooter was to develop the world's most efficient spectrograph in order to look deeper into the universe. The total efficiency of X-shooter NIR Spectrograph is calculated from optical efficiencies of broad band coatings on individual components (figure 17). The total efficiency is close to 40% including efficiency of the Telescope, dichroics in the backbone and detector quantum efficiency. The latest measurements at ESO seem to confirm a very high efficiency from 32% to 44%, but only on sky observations will give accurate and reliable results.

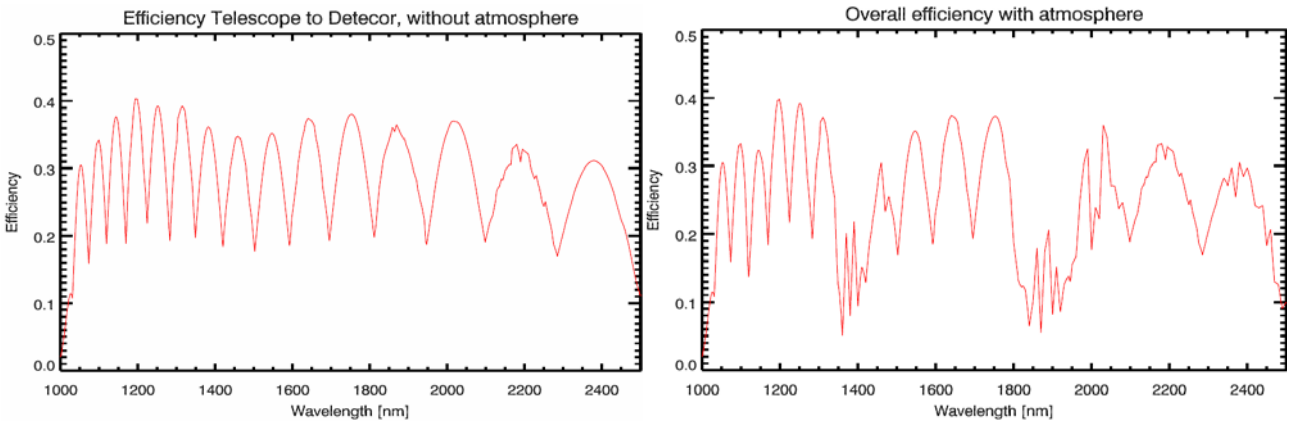

Figure 17. Efficiency of the X-shooter NIR spectrograph including efficiency of the Telescope, dichroics in the backbone and detector quantum efficiency. The efficiency is calculated from efficiencies of individual optical components and is shown without and with atmosphere transmission.

Electronic ghosts have been observed with light and dark edges, caused by crosstalk between adjacent amplifier channels in the detector (figure 18). The exact location of the ghosts can be predicted from the simultaneous readout of the 32 amplifiers. By running the amplifiers at half the speed (2.5 Mhz resulting in a full readout in ~ 1.7 sec) the effect could

be reduced by a factor of 10 and is no longer harmful in arc exposures; the impact of ghosts of sky lines will be evaluated during commissioning. Persistence, also known as remanence or latency, has been observed on the engineering grade detector. The magnitude of the effect depends greatly on the detector temperature: at 79 K persistence effects are virtually gone after a minute, while at 82 K the effect is still clearly visible after many hours. Optical ghosts were hardly observed, except for a defocused ghost located at 1012 nm, very close to the wavelength of the dichroic cutoff 1008 nm. The ghost level is 10^{-4} and appears only if the longer wavelengths are overexposed (figure 18).

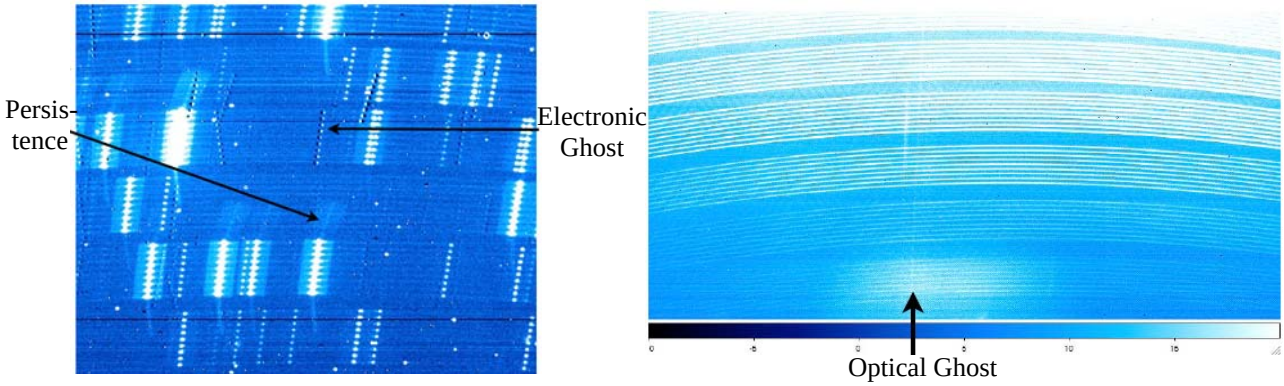

Figure 18. Electronic ghosts have been observed with light and dark edges, caused by crosstalk between adjacent amplifier channels in the detector. In the left image also persistence from a previous exposure with a wide slit and the rotation of the slit wheel can be observed. In the right image the only optical ghost is shown at a level of only 5 counts above the background. The ghost is located in order 26 at a wavelength of approximately 1012nm.

Flexure. A key aspect of any Cassegrain instrument is the stability of the location of the spectrum on the detector: the instrument flexure. In the design phase this has been extensively investigated as is shown in figure 19.

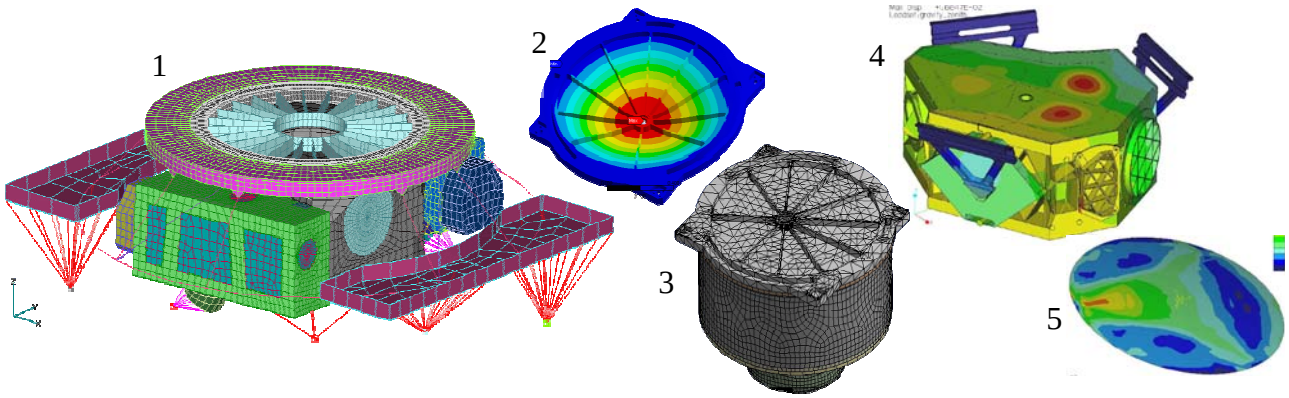

Figure 19. To predict instrument flexure behavior an extensive FEM analysis was performed during the design phase, consisting of 5 separate FEM models: The backbone[1], the NIR cryostat deformation due to air pressure[2] and gravity[3], the cold optics box[4] and individual mirrors[5]. The gravity direction is simulated at zenith and 12 rotation angles at 60° zenith distance.

Despite the fact that quite a few man years were spent in designing and constructing an extremely stiff structure to limit flexure effects, flexure is still out of the 1 pixel specification as is shown in figure 20. The largest impact of flexure on science performance is when subsequent images are subtracted in a nodding operation. Even flexure levels of 0.05 pixel can impact the data in this example and currently the nodding flexure is 0.08 pixel for the longest exposures possible (20 minutes). Measurements to find the root cause of the asymmetric flexure effect are continuing. Various possibilities for improvement are being investigated, including hardware repairs, instrument control options to circumvent the issue and software corrections on the acquired data.

Spectra of continuum sources showed extensive fringing, spaced at 4 - 8 pixels depending on wavelength, due to the 0.86 mm substrate on top of the Hawaii 2RG engineering chip with which the flexure tests were done. Fringing was completely eliminated after installing the final substrate-removed science detector.

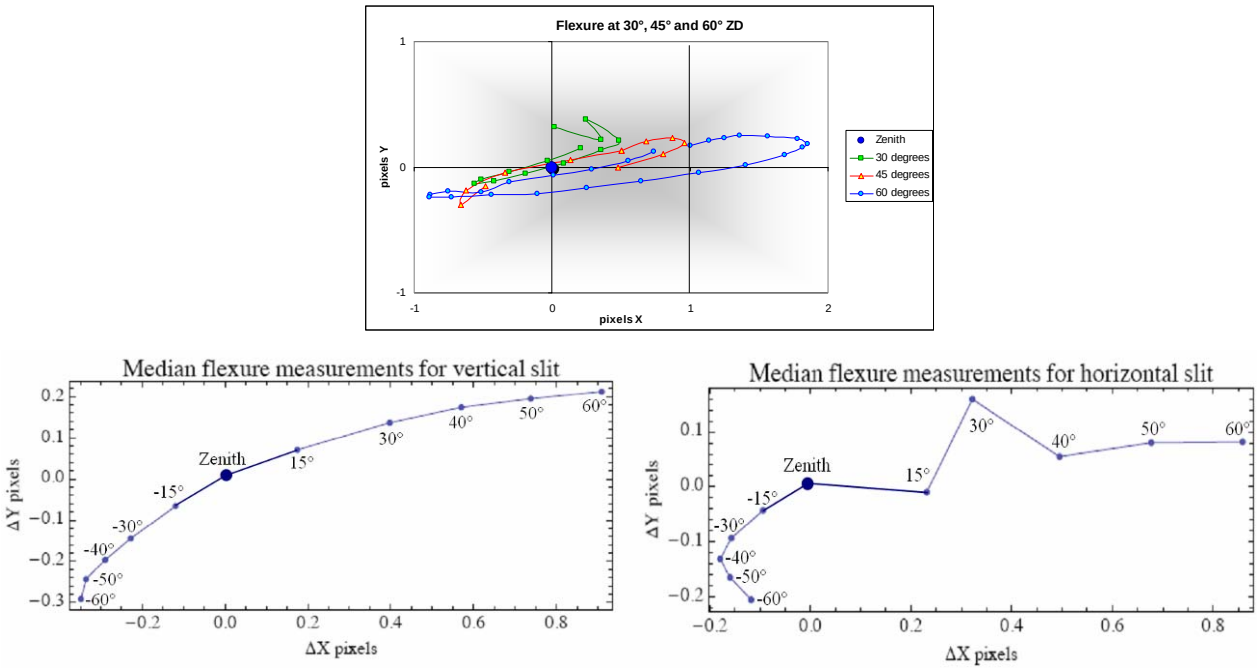

Figure 20. Flexure measured at various telescope and slit orientations. The flexure amounts more than 1 pixel at 60° Zenith distance (top figure). There is a preferred slit orientation to minimize flexure (left part in both bottom figures).

5. CONCLUSION

Several techniques have been developed at ASTRON in order to manufacture the X-shooter NIR Spectrograph to the sometimes conflicting specifications. The techniques discussed in this paper contribute to the performance of the instrument regarding mass, stiffness, deformation, position stability, stray light and cool down time.

The extra effort that was needed to design a virtually alignment-free integration of the instrument paid off. First light was achieved within seconds after integration and only 5 cool down runs were needed before acceptance of the instrument.

Despite the fact that quite a few man years were spent in designing and constructing an extremely stiff structure to limit flexure effects, at the moment flexure is out of specification. Several options are being investigated to reduce the effect.

ACKNOWLEDGEMENTS

This project is funded with contributions from NOVA, NWO, ASTRON, the University of Amsterdam and the Radboud University Nijmegen. The authors are grateful for the valuable contributions of ESO and the Danish, Italian and French partners of the X-shooter consortium.

REFERENCES

1. Sandro D'Odorico et al. X-shooter: a UV to K band, intermediate resolution VLT Spectrograph, Proceedings of SPIE, Vol. 6269-115, Orlando, 2006
2. Kaper, D'Odorico, Hammer, et al. 2008 X-shooter: a medium-resolution, wide band spectrograph for the VLT, in Proceedings 'Science with the VLT in the E-ELT era', Ed. A. Moorwood. (Astro-ph/08030609)
3. Ronald Roelfsema et al. X-shooter near-infrared spectrograph cryogenic design, SPIE Vol. 7017-44, Marseille, 2008
4. Paolo Spano et al. The optical design of X-shooter for the VLT, Proceedings of SPIE, Vol. 6269-107, Orlando, 2006
5. Ramon Navarro et al, X-shooter near-IR spectrograph arm: design and manufacturing methods, SPIE Vol. 6273-142, Orlando, 2006
6. Niels Tromp, ASTRON Extreme Light Weighting, Patent number: NL20021021771 20021029 / WO2004040349
7. Niels Tromp et al. ASTRON Extreme light Weighting, Proceedings of SPIE, Vol. 5495, Glasgow, 2004